Characterizing Topological Order by Studying the Ground States on an Infinite Cylinder

L. Cincio and G. Vidal

Perimeter Institute for Theoretical Physics, Waterloo, Ontario N2L 2Y5, Canada

(Received 13 August 2012; revised manuscript received 29 December 2012; published 7 February 2013)

Given a microscopic lattice Hamiltonian for a topologically ordered phase, we propose a numerical approach to characterize its emergent anyon model and, in a chiral phase, also its gapless edge theory. First, a tensor network representation of a complete, orthonormal set of ground states on a cylinder of infinite length and finite width is obtained through numerical optimization. Each of these ground states is argued to have a different anyonic flux threading through the cylinder. Then a quasiorthogonal basis on the torus is produced by chopping off and reconnecting the tensor network representation on the cylinder. From these two bases, and by using a number of previous results, most notably the recent proposal of Y. Zhang *et al.* [Phys. Rev. B **85**, 235151 (2012)] to extract the modular U and S matrices, we obtain (i) a complete list of anyon types i, together with (ii) their quantum dimensions d_i and total quantum dimension D, (iii) their fusion rules $N_{ij}{}^{k}$, (iv) their mutual statistics, as encoded in the off-diagonal entries S_{ij} of S, (v) their self-statistics or topological spins θ_i, (vi) the topological central charge c of the anyon model, and, in a chiral phase (vii) the low energy spectrum of each sector of the boundary conformal field theory. As a concrete application, we study the hard-core boson Haldane model by using the two-dimensional density matrix renormalization group. A thorough characterization of its universal bulk and edge properties unambiguously shows that it realizes a $\nu = 1/2$ bosonic fractional quantum Hall state.

DOI: 10.1103/PhysRevLett.110.067208 PACS numbers: 75.10.Kt, 03.67.−a

Introduction.—Determining the emergent order of an interacting quantum many-body system from its microscopic description is one of the main goals of condensed matter theory. It is also an extremely challenging problem. Consider, for instance, a lattice Hamiltonian H suspected of realizing some form of topological order [1], say a given Laughlin state [2] or a quantum spin liquid [3,4]—states of considerable interest in the study of exotic many-body phenomena, such as the fractional quantum Hall (FQH) effect [5], and in the design of a quantum computer protected from decoherence by topology [6,7]. Due to a lack of theoretical and computational tools, assessing whether the Hamiltonian H is indeed topologically ordered, and then establishing what type of topological order it realizes, have traditionally been considered very difficult tasks. However, recent advances in the understanding of many-body entanglement have progressively brought us closer to being able to tackle such questions. On the theoretical side, new ways of diagnosing the presence and type of topological order from knowledge of the ground state wave function alone, based on entanglement entropy [8–10], entanglement spectrum [11,12], and modular transformations [13,14], have been put forward. On the computational side, the advent of tensor networks [15–21] makes it now possible, by mimicking the structure of entanglement, to efficiently represent a large class of low energy many-body states.

In this Letter, we combine and build upon the above developments [8–21] to produce an approach that, given a microscopic Hamiltonian H on a two-dimensional lattice, characterizes its emergent topological order. The key of our approach is the numerical computation of a basis of ground states of H, first on an infinite cylinder, then on a finite torus. Each ground state has a different anyon flux through the cylinder or torus, so that ground states are in one-to-one correspondence with types of anyons in the emergent anyon model. These ground states are encoded in a tensor network representation, from which we can extract the universal properties of the emergent edge and bulk theories. For concreteness, we focus on a specific lattice Hamiltonian, namely the Haldane model on the honeycomb lattice [22] with hard-core bosons [23],

$$H_{\mathrm{Hal.}} = -t\sum_{\langle rr'\rangle} b_r^\dagger b_{r'} - t'\sum_{\langle\langle rr'\rangle\rangle} b_r^\dagger b_{r'} e^{i\phi_{rr'}} - t''\sum_{\langle\langle\langle rr'\rangle\rangle\rangle} b_r^\dagger b_{r'} + \mathrm{H.c.}, \quad (1)$$

where we set $\phi = 0.4\pi$ and $(t, t', t'') = (1, 0.6, -0.58)$, and where t, t', and t'' stand for the hoping amplitudes between nearest, next-nearest, and next-next-nearest neighbors, respectively. For these parameters, Ref. [23] found two quasidegenerate ground states and a nontrivial Chern number $C = 1$ using exact diagonalization on small tori, while Ref. [20] computed a nonzero topological entanglement entropy (TEE) [8,9] $\gamma \approx \log\sqrt{2}$ by studying finite cylinders with the density matrix renormalization group (DMRG) [15]. These results strongly indicate the presence of topological order and are suggestive of a $\nu = 1/2$ bosonic FQH state [2,24]. Such a state would have a chiral semion [25] in the bulk and a $SU(2)_1$ Wess-Zumino-Witten conformal field theory (CFT) [26] at the edge. Here, without making

use of any previous knowledge about $H_{\text{Hal.}}$, we produce a detailed characterization of both bulk and edge theories and therefore unambiguously demonstrate the emergence of a $\nu = 1/2$ bosonic FQH state. Our approach can be readily applied to other Hamiltonians on honeycomb, triangular, and kagome lattices (with $\pi/3$ rotational symmetry), and can be generalized to arbitrary lattices (even without any rotational symmetry) [27].

Ground states on an infinite cylinder.—Our goal is to investigate a generic microscopic lattice model realizing a topologically ordered phase, as characterized by an emergent anyon model with N types of anyon flux. For this purpose, we define the model on a cylinder of size $L_x \times L_y$, as measured in lattice unit cells, with infinite length $L_x = \infty$ and finite width L_y; see Fig. 1(a).

Let us first consider the ground subspace of a fixed-point Hamiltonian $H^{(0)}$, with a vanishing correlation length $\xi^{(0)} = 0$. This ground subspace is spanned by N orthonormal states $\{|\Psi_i^{\text{cyl}(0)}\rangle\}$, where state $|\Psi_i^{\text{cyl}(0)}\rangle$ has anyon type i threading through the cylinder. Notice the one-to-one correspondence with the N ground states of $H^{(0)}$ on a torus [1]. (An infinite torus can be obtained by identifying the $x = \pm\infty$ ends of the infinite cylinder. The absence of boundaries on an infinite cylinder, which could assign different boundary energies to each anyon flux i, is essential in order to establish the N-fold ground state degeneracy.) Let us now consider a more realistic Hamiltonian H for the same topological phase, with $H = H^{(0)} + V$ for some perturbation V that decomposes into sum of local terms. Perturbation V introduces a finite correlation length $\xi > 0$. Following Ref. [6], for $L_y \gg \xi$ we expect degenerate perturbation theory to apply. Because L_x is infinite, at any finite order in a perturbative expansion, virtual anyon pairs created, propagated, and annihilated by V can only close a nontrivial loop in the $\hat{y}$ direction. These virtual pairs may renormalize the energy of each ground state by an amount that depends on the anyon flux i threading through the cylinder, but they cannot change this flux. The net result is that the state $|\Psi_i^{\text{cyl}}\rangle$, obtained from $|\Psi_i^{\text{cyl}(0)}\rangle$ by adiabatically switching on perturbation V, is an eigenstate of H with anyonic flux i, as measured by a *dressed* Wilson loop operator [28] encircling the cylinder in the $\hat{y}$ direction. Correspondingly, we refer to $|\Psi_i^{\text{cyl}}\rangle$ as the ground state of H with flux i through the cylinder. Notice that the energy per unit cell, $e_i \equiv \langle\Psi_i^{\text{cyl}}|H|\Psi_i^{\text{cyl}}\rangle/(L_x L_y)$, satisfies $e_i - e_j \approx e^{-L_y/\xi}$ [6]. Reference [19] already pointed out that the absolute ground state of H on a sufficiently long cylinder has well-defined anyon flux (of some unknown type) through it. Above we argued that actually each of the N quasidegenerate ground states $|\Psi_i^{\text{cyl}}\rangle$ has this property, which is key to the present approach.

Tensor network approach.—As a variational ansatz for each ground state $|\Psi_i^{\text{cyl}}\rangle$ of H on a cylinder, we employ a matrix product state (MPS) optimized using DMRG [15], as in previous finite cylinder calculations [18–21]. Here, however, we use an infinite MPS, characterized by a finite unit cell of tensors that are repeated throughout the infinite cylinder [see Fig. 2(a)] and an infinite DMRG algorithm [29,30] adapted to cylinders, as detailed in Ref. [27]. The computational cost scales exponentially with the width L_y of the cylinder. As a result, only small values of L_y can be

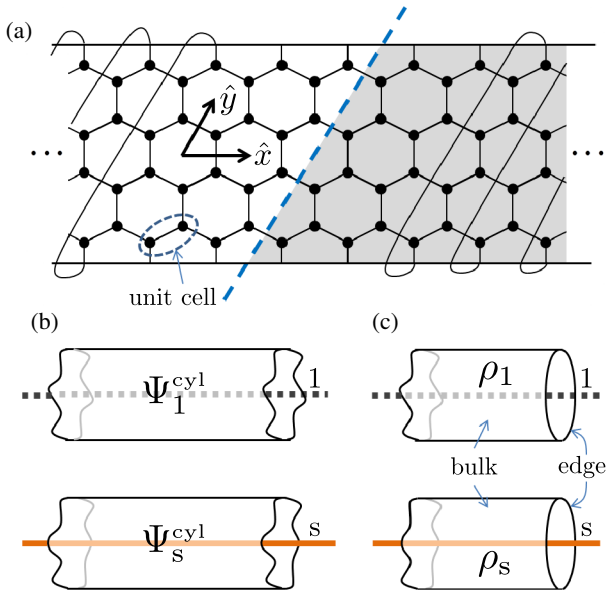

FIG. 1 (color online). (a) Honeycomb lattice on a cylinder with $L_x = \infty$ and $L_y = 4$ (as measured in number of unit cells). A blue, dashed line indicates the entanglement cut used in dividing the cylinder into two semi-infinite cylinders. (b) Ground states $|\Psi_1^{\text{cyl}}\rangle$ and $|\Psi_s^{\text{cyl}}\rangle$ of $H_{\text{Hal.}}$ in Eq. (1) with flux $i = 1, s$. (c) Corresponding density matrices ρ_1 and ρ_s for the left half of the infinite cylinder.

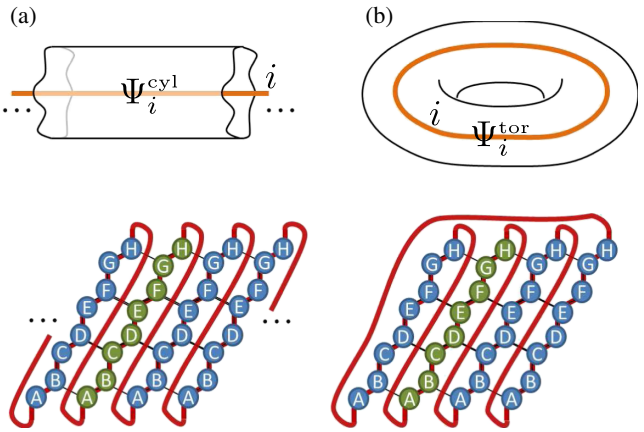

FIG. 2 (color online). (a) MPS representation of a state $|\Psi_i^{\text{cyl}}\rangle$ of an infinite cylinder with $L_y = 4$; see Fig. 1(a). The bond indices that connect tensors form a snake. The MPS unit cell consists of eight tensors that are repeated indefinitely. (b) Periodic MPS for a state $|\Psi_i^{\text{tor}}\rangle$ of a torus with $4 \times 4 \times 2 = 32$ sites, obtained by reconnecting four MPS unit cells of $|\Psi_i^{\text{cyl}}\rangle$.

considered. To ensure small finite size effects, we would like to have $L_y \gg \xi$.

Specifically, we have analyzed the Hamiltonian $H_{\text{Hal.}}$ of Eq. (1) on infinite cylinders of width $L_y = 4$, 6, and 8. For each width L_y, we repeated the optimization of infinite MPS several times, starting from random variational parameters. Each energy minimization arbitrarily produced one of two states, which we denote $|\Psi_1^{\text{cyl}}\rangle$ and $|\Psi_s^{\text{cyl}}\rangle$, anticipating that they correspond to anyon types $i = 1$, or *identity* charge, and $i = s$, or *semion* charge, respectively. (This will be confirmed later.) We conclude that $H_{\text{Hal.}}$ has at least two ground states or, equivalently, that the emergent anyon model has $N \geq 2$ anyon charges. A correlation length $\xi \approx 0.52$ for both states, computed from a transfer matrix, verifies that $\xi/L_y \approx 0.065 \ll 1$, and thus we expect small finite size effects.

Next, we cut and reconnect the MPS representation for the ground state $|\Psi_i^{\text{cyl}}\rangle$ on an infinite cylinder to obtain a (periodic) MPS for a state $|\Psi_i^{\text{tor}}\rangle$ on a finite torus, as illustrated in Fig. 2. Crucially, state $|\Psi_i^{\text{tor}}\rangle$ inherits the property of having an anyon of type i threading inside the torus; see Fig. 2(b). The rest of this Letter explains how, with the states $\{|\Psi_i^{\text{cyl}}\rangle\}$ and $\{|\Psi_i^{\text{tor}}\rangle\}$ for an infinite cylinder and a finite torus, one can use the results of Refs. [8–14] to characterize in great detail the anyon model emerging from Hamiltonian $H_{\text{Hal.}}$.

Entanglement spectrum and entanglement entropy.—The tensor network for state $|\Psi_i^{\text{cyl}}\rangle$ on the infinite cylinder readily provides access to the eigenvalues $\{p_{i,\alpha}\}$ of the reduced density matrix ρ_i for a semi-infinite cylinder; see Fig. 1(c). The corresponding entanglement spectrum (ES) [11,12], plotted in Fig. 3, reveals that each ground state of $H_{\text{Hal.}}$ is associated with one of the two primary fields of the chiral $SU(2)_1$ Wess-Zumino-Witten CFT [26], namely the identity operator and the chiral boson vertex operator $e^{i\phi/\sqrt{2}}$, which are seen to be a singlet and a doublet of an emergent $SU(2)$ symmetry. Specifically, the ES of $|\Psi_1^{\text{cyl}}\rangle$ is organized according to the scaling dimensions and conformal spins of the identity primary field of this CFT and of its tower of (Kac-Moody and Virasoro) descendants, whereas the ES of $|\Psi_s^{\text{cyl}}\rangle$ corresponds to operator $e^{i\phi/\sqrt{2}}$ and its descendants, which justifies our previous identification of $|\Psi_1^{\text{cyl}}\rangle$ and $|\Psi_s^{\text{cyl}}\rangle$ with the anyonic charges $i = 1$ and s, respectively. Thus, from the ES of $\{|\Psi_i^{\text{cyl}}\rangle\}$ we have unambiguously identified the edge CFT of the emergent anyon model. Furthermore, from the entropy $S(\rho_i) \equiv -\sum_\alpha p_{i\alpha} \log(p_{i\alpha})$, which scales with L_y as $\alpha L_y - \gamma_i$ [8,9], we can also estimate the TEE γ_i for $|\Psi_i^{\text{cyl}}\rangle$. We obtain $\gamma_1 \approx 0.3455$, $\gamma_s \approx 0.986 \times \gamma_1$, very similar to the finite cylinder result (for just one ground state) of Ref. [20], where the same type of *corner-free* bipartition of a cylinder was first considered. The expression [8,10]

$$\gamma_i = -\log(d_i/D), \qquad D \equiv \sqrt{\sum_i (d_i)^2}, \tag{2}$$

allows us then to compute each *quantum dimension* d_i and the *total quantum dimension* D as follows. First, we note that the sum $\sum_i (d_i/D)^2$, made of positive contributions, only reaches unity when it includes all the anyon types. We can use this sum to determine whether we have obtained a complete set of ground states. Our estimates of γ_i yield $(d_1/D)^2 + (d_s/D)^2 \approx 1.007$. We conclude that $H_{\text{Hal.}}$ only has two ground states; i.e., the emergent anyon model has $N = 2$ types of anyons, in agreement with exact results for small tori [23]. We then use the fact that any anyon model has the identity flux, with quantum dimension $d_1 = 1$, to numerically obtain the quantum dimension $d_s = 1.005$ from $\gamma_s - \gamma_1 = -\log(d_s/d_1)$, and the total quantum dimension $D = 1.413$ from $\gamma_1 = -\log(d_1/D)$. These values are very close to the exact $d_s = 1$ and $D = \sqrt{2} \approx 1.414$ of the semion model [25].

Modular U and S matrices.—Next we use the states $\{|\Psi_i^{\text{tor}}\rangle\}$ on a finite torus to compute, following Ref. [13], the modular matrices S and U that characterize the mutual and self-statistics of the emergent anyon model [31],

$$S = \begin{bmatrix} S_{11} & S_{1s} \\ S_{s1} & S_{ss} \end{bmatrix}, \qquad U = e^{-i(2\pi/24)c} \begin{bmatrix} \theta_1 & 0 \\ 0 & \theta_s \end{bmatrix}. \tag{3}$$

Here, $S_{1i} = S_{i1} = d_i/D$ and the entry S_{ij} determines (for any Abelian anyon model) the phase acquired when an anyon of type i encircles an anyon of type j, c is the central charge of the anyon model, and θ_i corresponds to the phase acquired when an anyon of type i is exchanged with another anyon of type i (and thus $\theta_1 = 1$).

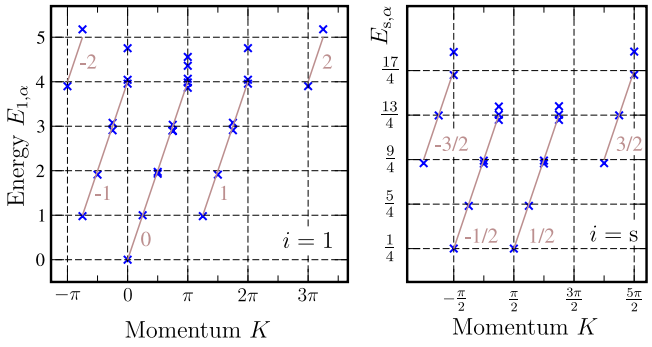

FIG. 3 (color online). Entanglement spectrum of the reduced density matrix ρ_i for half an infinite cylinder for ground state $|\Psi_i^{\text{cyl}}\rangle$, for $i = 1$ (left) and s (right). The vertical axis shows $E_{i,\alpha} \equiv -\log(p_{i,\alpha})$ (up to a global shift and rescaling), where $\{p_{i,\alpha}\}$ are the eigenvalues of ρ_i. The horizontal axis shows the momentum of the corresponding eigenvector of ρ_i, artificially extended beyond its 2π periodicity. All eigenvalues of ρ_i with the same particle number (also indicated) are connected with a tilted line. They obey the degeneracy pattern $\{1, 1, 2, 3, 5, \cdots\}$, characteristic of a bosonic Gaussian theory.

A $\pi/3$ clockwise rotation $R_{\pi/3}$ on the torus corresponds to applying the modular transformation $\mathfrak{u}\mathfrak{s}^{-1}$, where $\mathfrak{u}$ and $\mathfrak{s}$ generate the group of modular transformations on the torus [13]. Correspondingly, the overlaps $V_{ij} \equiv \langle \Psi_i^{\text{tor}} | R_{\pi/3} | \Psi_j^{\text{tor}} \rangle$ between the bases $\{|\Psi_i^{\text{tor}}\rangle\}$ and $\{R_{\pi/3}|\Psi_j^{\text{tor}}\rangle\}$ define a unitary transformation $V = D^\dagger U S^{-1} D$. Here, D is a diagonal matrix that contains arbitrary phases $D_{jj} = e^{i\phi_j}$ (due to the phase freedom in choosing each $|\Psi_j^{\text{tor}}\rangle$), and S and U generate a representation of the modular group on the ground subspace of $H_{\text{Hal.}}$. We find

$$V = e^{-i(2\pi/24)c} \begin{bmatrix} S_{11} & S_{s1} e^{i(\phi_s - \phi_1)} \\ S_{1s}\theta_s e^{i(\phi_1 - \phi_s)} & (S_{ss})^* \theta_s \end{bmatrix}, \quad (4)$$

$$= \begin{bmatrix} 0.683 - 0.183i & -0.696 + 0.137i \\ -0.228 - 0.671i & -0.185 - 0.683i \end{bmatrix}, \quad (5)$$

where in the first line we use that $S_{1i}, S_{i1} > 0$, $S^{-1} = S^\dagger$, and $\theta_1 = 1$, whereas the second line shows the overlaps V_{ij} for a torus made of $6 \times 6 \times 2 = 72$ sites, computed from the periodic MPS representations using Monte Carlo sampling [32], with sampling noise on the order of 10^{-4}. Building on Ref. [13], here we note that from matrix V we can actually compute *both* U and S. Indeed, from V_{11} we obtain the central charge c and S_{11}; then from V_{1s} we read $e^{i(\phi_s - \phi_1)}$ and S_{s1}; from V_{s1} we extract θ_s and S_{1s}; finally, V_{ss} yields S_{ss}. We thus obtain

$$S = \frac{1}{\sqrt{2}} \begin{bmatrix} 1 & 1 \\ 1 & -1 \end{bmatrix} + \frac{10^{-3}}{\sqrt{2}} \begin{bmatrix} -1.4 & 0.07 \\ -0.8 & 4 + 4i \end{bmatrix}, \quad (6)$$

$$U = e^{-i(2\pi/24)} \begin{bmatrix} 1 & 0 \\ 0 & i \end{bmatrix} \times \left(e^{i(2\pi/24)0.01} \begin{bmatrix} 1 & 0 \\ 0 & e^{-i0.007} \end{bmatrix} \right), \quad (7)$$

which accurately reproduce the exact S and U of a chiral semion model, namely

$$\frac{1}{\sqrt{2}} \begin{bmatrix} 1 & 1 \\ 1 & -1 \end{bmatrix}$$

and

$$e^{-i(2\pi/24)} \begin{bmatrix} 1 & 0 \\ 0 & i \end{bmatrix}.$$

Properties (i)–(vi) of the emergent anyon model listed in the abstract can now be extracted from Eqs. (6) and (7) as follows. The first row and column of S correspond to $S_{1i} = S_{i1} = d_i/D$. Therefore, Eq. (6) gives us an estimate for each d_i/D [Notice that these estimates are independent from those obtained through the TEE of Eq. (2).] We can then repeat the argument used before to conclude that there are (i) $N = 2$ types of anyons, which we label $i = \{1, s\}$, with (ii) quantum dimensions $d_1 = d_s = 1$ and total quantum dimension $D = \sqrt{2}$, up to 10^{-3} corrections. Verlinde formula $N_{ij}{}^k = \sum_m (S_{im} S_{jm} (S_{mk})^* / S_{1m})$ [33] then reproduces (iii) the $\mathbb{Z}_2$ fusion rules, $1 \times 1 = s \times s = 1, 1 \times s = s \times 1 = s$, whereas (iv) the mutual statistics are seen to be trivial, as expected since they always involve the identity flux. Further, from Eq. (7) we find (v) topological twists $\theta_1 = 1$ and $\theta_s = i$, characteristic of identity and semion fluxes, and (vi) central charge $c = 1$ (modulus 24), up to 10^{-2} corrections. From the above list of properties, only the degeneracy $N = 2$ and the total quantum dimension $D = \sqrt{2}$ were previously computed (with exact diagonalization on small tori [23] and DMRG on finite cylinders [20], respectively), which showcases the power of studying ground states on an infinite cylinder instead.

In summary, we have proposed an approach to numerically obtain a complete set of ground states of a microscopic lattice Hamiltonian H with emergent topological order. In the infinite cylinder geometry, each of the ground states was argued to have a different anyon flux threading through the cylinder. By cutting and reconnecting their tensor network representation, we also obtained analogous states on a finite torus. From these two sets of states, we then extracted a very fined grained characterization of the emergent anyon model using Refs. [8–14]. The major bottleneck of the approach, in the DMRG implementation discussed here, is a computational cost that grows exponentially with the width L_y of the cylinder, so that only certain values of L_y (up to $L_y = 8$ in our example) can be afforded. It implies that only models with a small correlation length ξ, such that $\xi \ll L_y$, can be consistently analyzed. To overcome this limitation, we are currently adapting scalable 2D tensor network approaches [16,17] to infinite cylinders [27]. Finally, in this Letter we have only extracted properties of the emergent anyon model that are directly available from ground states of H. With further manipulation, it is also possible to obtain an explicit representation of fractionalized quasiparticle excitations of H [27].

The authors thank Jaume Gomis and Xiao-Gang Wen for guidance in identifying the edge theory resulting from the numerical simulations, and Oliver Buerschaper, Tarun Grover, Todadri Senthil, and Ashvin Vishwanath for insightful discussions.

[1] X.-G. Wen, Int. J. Mod. Phys. B **04**, 239 (1990).
[2] R. B. Laughlin, Phys. Rev. Lett. **50**, 1395 (1983).
[3] P. W. Anderson, Mater. Res. Bull. **8**, 153 (1973).
[4] L. Balents, Nature (London) **464**, 199 (2010).
[5] D. C. Tsui, H. L. Stormer, and A. C. Gossard, Phys. Rev. Lett. **48**, 1559 (1982).
[6] A. Y. Kitaev, Ann. Phys. (Amsterdam) **303**, 2 (2003).
[7] C. Nayak, S. H. Simon, A. Stern, M. Freedman, and S. Das Sarma, Rev. Mod. Phys. **80**, 1083 (2008).
[8] A. Kitaev and J. Preskill, Phys. Rev. Lett. **96**, 110404 (2006).
[9] M. Levin and X.-G. Wen, Phys. Rev. Lett. **96**, 110405 (2006).

[10] S. Dong, E. Fradkin, R. G. Leigh, and S. Nowling, J. High Energy Phys. 05 (2008) 016.
[11] H. Li and F. D. M. Haldane, Phys. Rev. Lett. **101**, 010504 (2008).
[12] X.-L. Qi, H. Katsura, and A. W. W. Ludwig, Phys. Rev. Lett. **108**, 196402 (2012).
[13] Y. Zhang, T. Grover, A. Turner, M. Oshikawa, and A. Vishwanath, Phys. Rev. B **85**, 235151 (2012).
[14] T. Grover, arXiv:1112.2215v1.
[15] S. R. White, Phys. Rev. Lett. **69**, 2863 (1992); Phys. Rev. B **48**, 10345 (1993).
[16] F. Verstraete and J. I. Cirac, arXiv:cond-mat/0407066v1; J. Jordan, R. Orus, G. Vidal, F. Verstraete, and J. I. Cirac, Phys. Rev. Lett. **101**, 250602 (2008).
[17] G. Vidal, Phys. Rev. Lett. **99**, 220405 (2007); M. Aguado and G. Vidal, Phys. Rev. Lett. **100**, 070404 (2008).
[18] S. Yan, D. A. Huse, and S. R. White, Science **332**, 1173 (2011).
[19] H.-C. Jiang, H. Yao, and L. Balents, Phys. Rev. B **86**, 024424 (2012).
[20] H.-C. Jiang, Z. Wang, and L. Balents, Nat. Phys. **8**, 902 (2012).
[21] S. Depenbrock, I. P. McCulloch, and U. Schollwöck, Phys. Rev. Lett. **109**, 067201 (2012).
[22] F. D. M. Haldane, Phys. Rev. Lett. **61**, 2015 (1988).
[23] Y.-F. Wang, Z.-C. Gu, C.-D. Gong, and D. N. Sheng, Phys. Rev. Lett. **107**, 146803 (2011).
[24] V. Kalmeyer and R. B. Laughlin, Phys. Rev. Lett. **59**, 2095 (1987).
[25] P. Bonderson, Ph.D. thesis, Caltech, 2007, http://thesis.library.caltech.edu/2447/2/thesis.pdf.
[26] P. Di Francesco, P. Mathieu, and D. Senechal, *Conformal Field Theory* (Springer, New York, 1997), Chap. 15.6.
[27] L. Cincio *et al.* (to be published).
[28] M. B. Hastings and X.-G, Wen, Phys. Rev. B **72**, 045141 (2005).
[29] I. P. McCulloch, arXiv:0804.2509v1.
[30] G. M. Crosswhite, A. C. Doherty, and G. Vidal, Phys. Rev. B **78**, 035116 (2008).
[31] See Supplemental Material at http://link.aps.org/supplemental/10.1103/PhysRevLett.110.067208 for extended explanations and technical details of the approach.
[32] A. W. Sandvik and G. Vidal, Phys. Rev. Lett. **99**, 220602 (2007).
[33] E. Verlinde, Nucl. Phys. **B300**, 360 (1988).